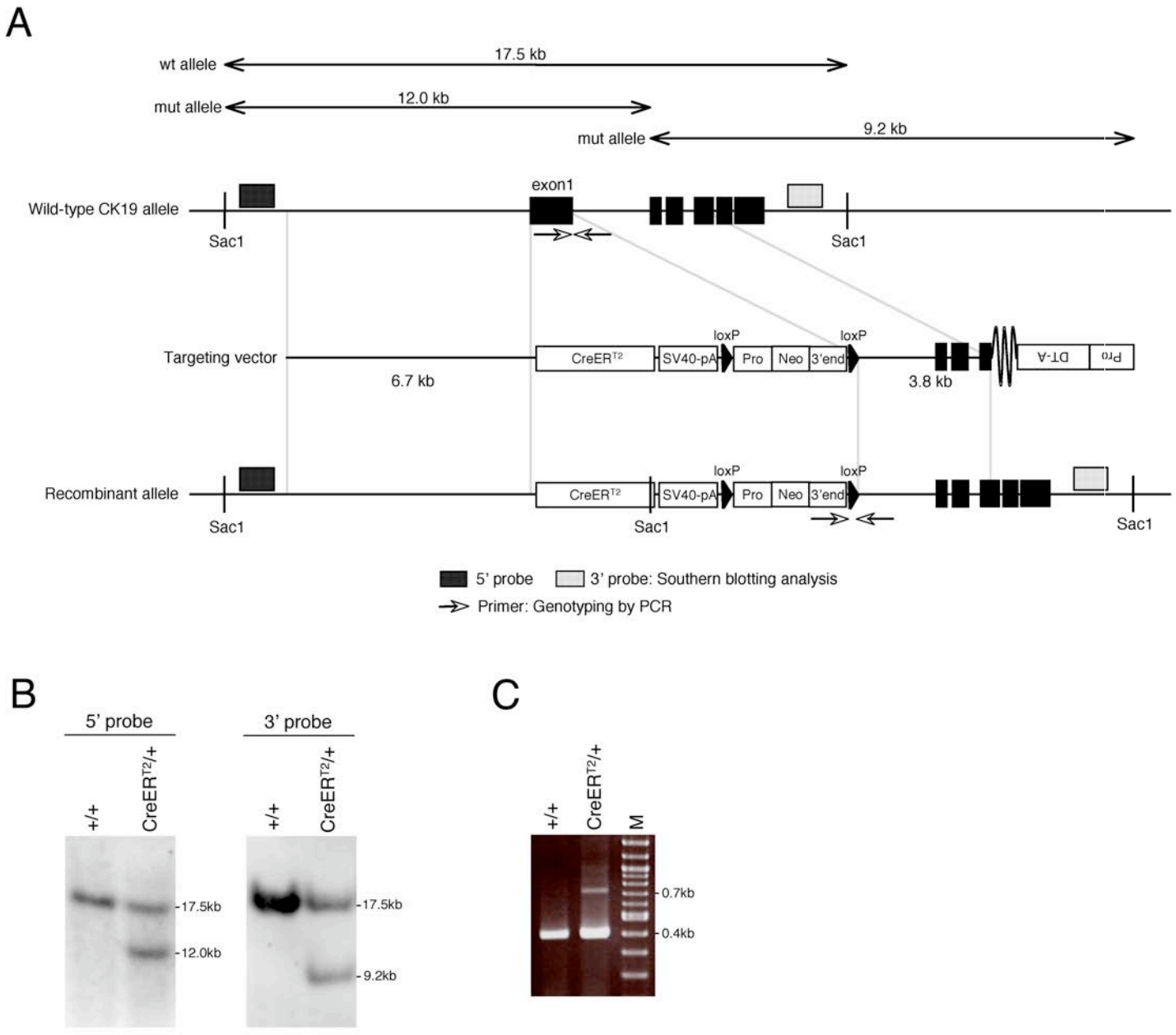

Supplemental Figure 1 Targeting strategy for producing the *CK19-CreER^{T2}* knock-in allele. (**A**) Targeted insertion of the CreER^{T2} coding sequence into the first exon of the *CK19* gene by homologous recombination in embryonic stem cells. (**B**) Genomic Southern blotting analyses of parental and targeted embryonic stem cells using 5' and 3' probes. (**C**) PCR genotyping using genomic DNA from tail snips obtained from wild-type and *CK19-CreER^{T2}* heterozygous mice. M, markers.

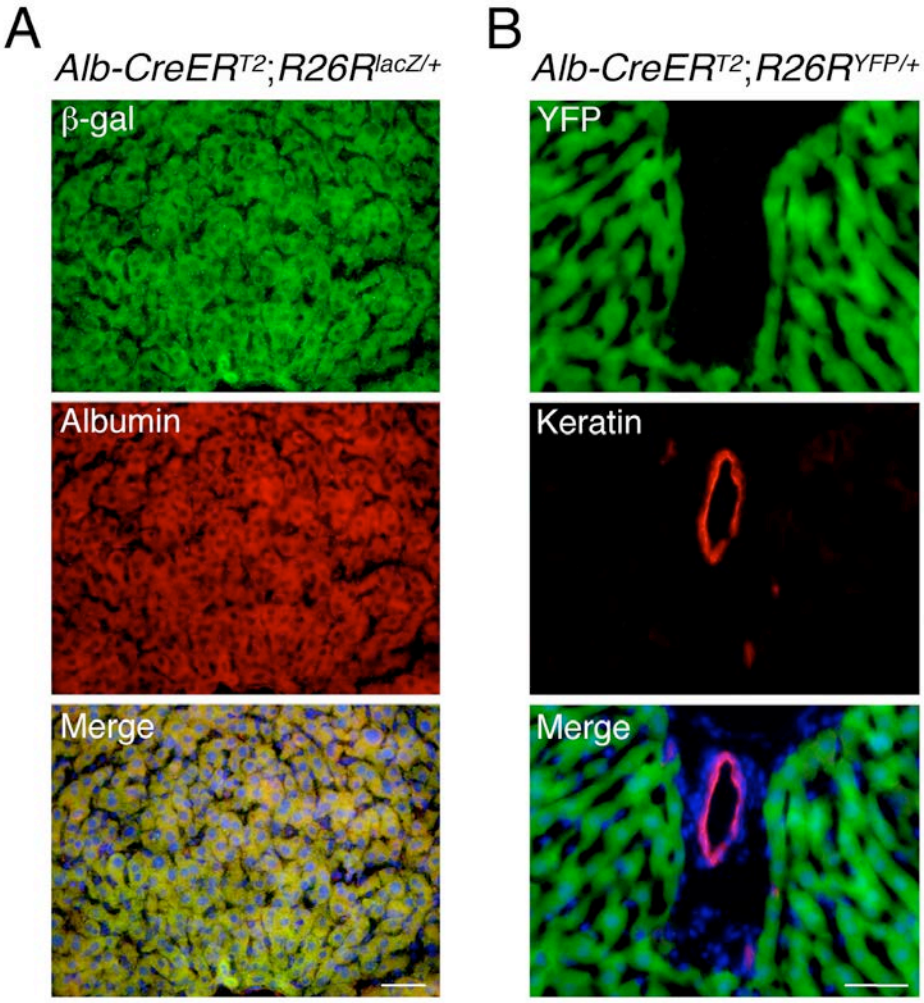

Supplemental Figure 2 Genetic marking of *albumin*-expressing hepatocytes in the adult mouse liver. (**A**) Co-immunofluorescence staining of β-gal and albumin was conducted in the liver of *Alb-CreER*^{T2};*R26R*$^{lacZ/+}$ mice at 1 week after TM injection. Yellow signals indicate merged red and green signals (bottom panel). (**B**) Immunofluorescence staining of the cholangiocyte marker keratin was conducted in the liver of *Alb-CreER*^{T2};*R26R*$^{YFP/+}$ mice at 1 week after TM injection. YFP expression is induced in hepatocytes, but not in keratin-positive cholangiocytes. DNA was stained with DAPI. Scale bars, 50 μm.

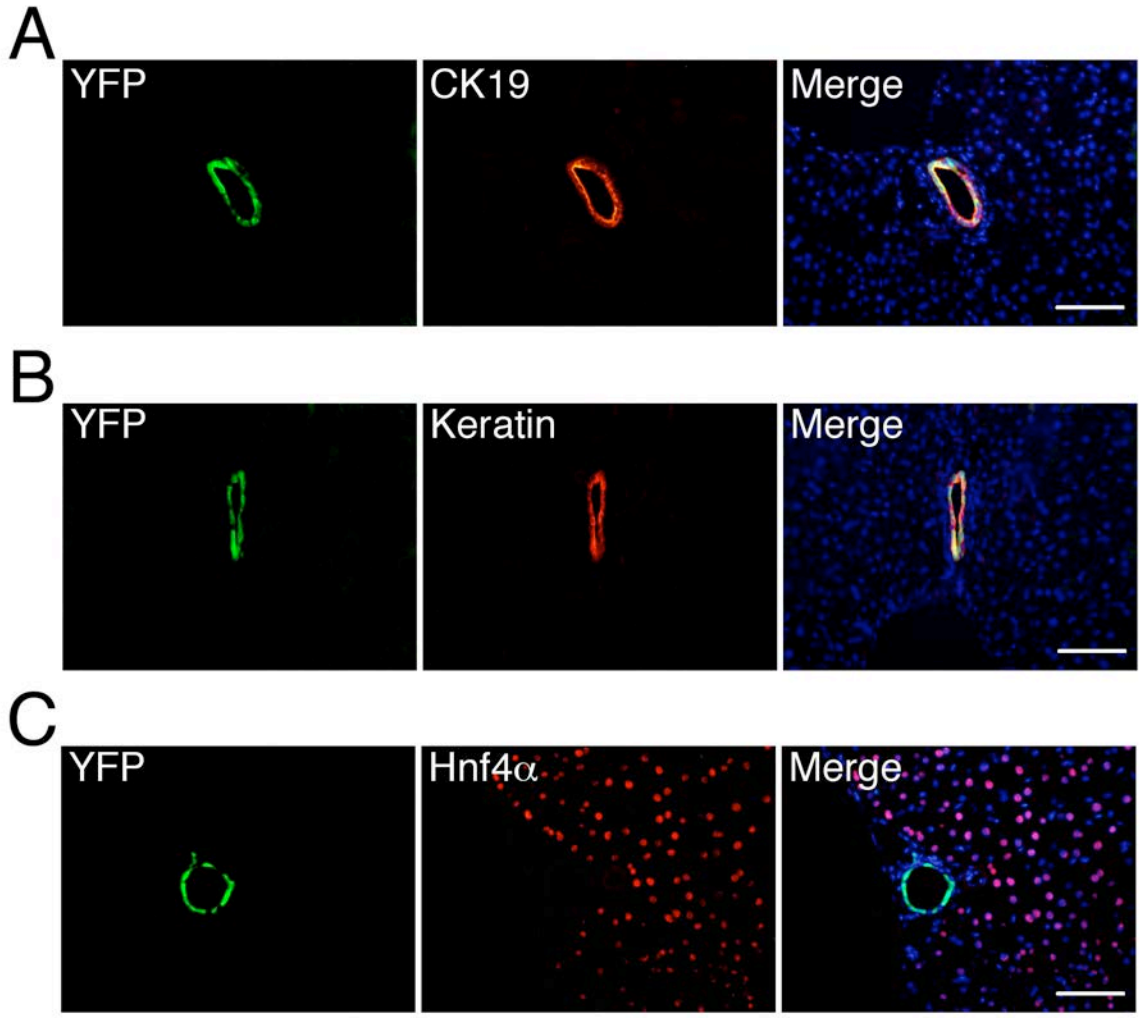

Supplemental Figure 3 Genetic marking of *CK19*-expressing cholangiocytes in the adult mouse liver. (**A**–**C**) Immunofluorescence staining of CK19 (**A**), keratin (**B**) and Hnf4α (**C**) were conducted in the liver of *CK19-CreER*^{T2};*R26R*$^{YFP/+}$ mice at 1 week after TM injection. YFP expression is induced in cholangiocytes, but not in Hnf4α-positive hepatocytes. DNA was stained with DAPI. Scale bars, 100 μm.

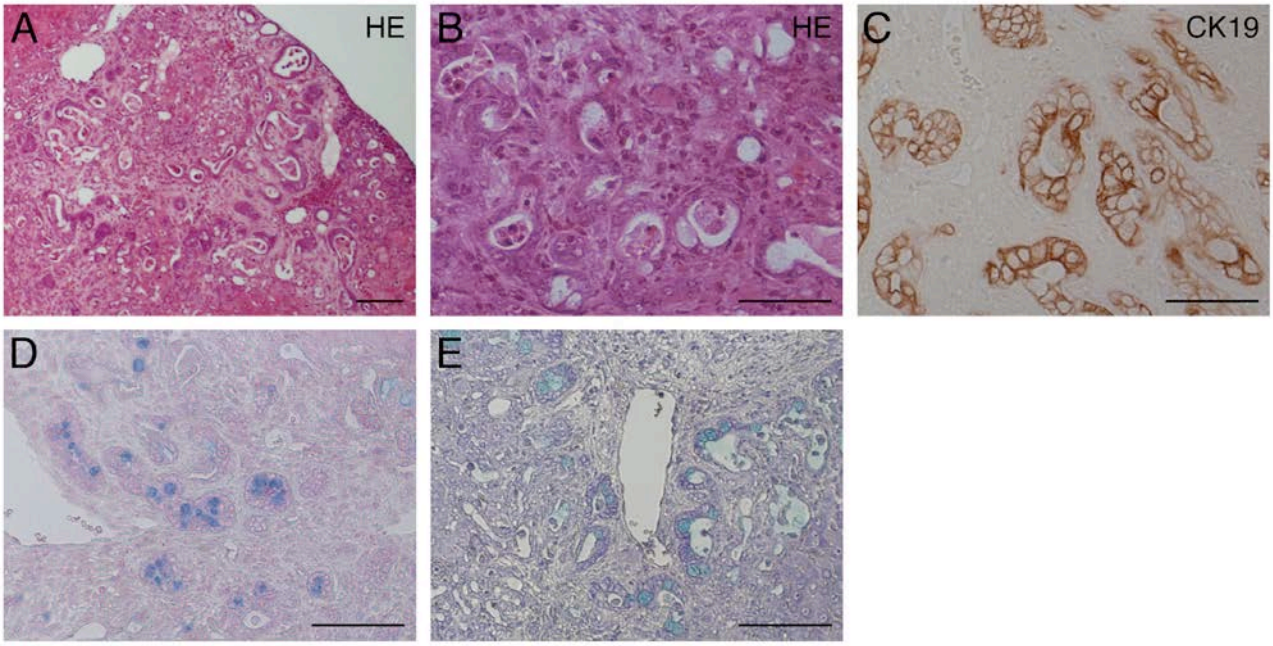

Supplemental Figure 4 Histological, immunohistochemical and histochemical analyses of neoplastic nodules formed in the liver after 30 weeks of TAA administration. (**A**–**E**) Hematoxylin and eosin (HE) staining (**A** and **B**), immunohistochemical staining of CK19 (**C**) and alcian blue staining with nuclear fast red (**D**) or hematoxylin (**E**) counterstaining were conducted for neoplastic nodules formed in the liver. Scale bars, 100 μm (**A, D** and **E**) and 50 μm (**B** and **C**).

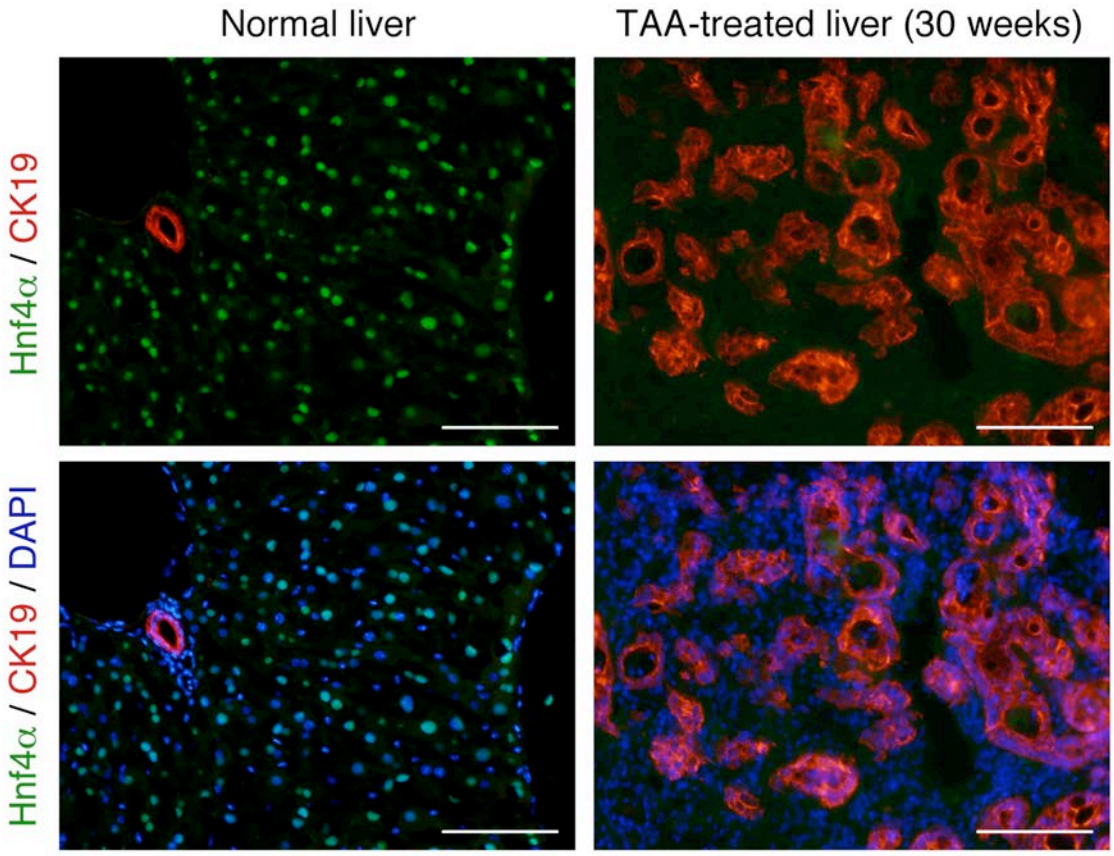

Supplemental Figure 5 The absence of Hnf4α expression in primitive ductular cells eliminates the possibility of the development of hepatocellular carcinoma with pseudoglandular formation after 30 weeks of TAA administration. Co-immunofluorescence staining of Hnf4α and CK19 was conducted for normal (left panels) or TAA-treated (right panels) livers. DNA was stained with DAPI. Scale bars, 100 μm.

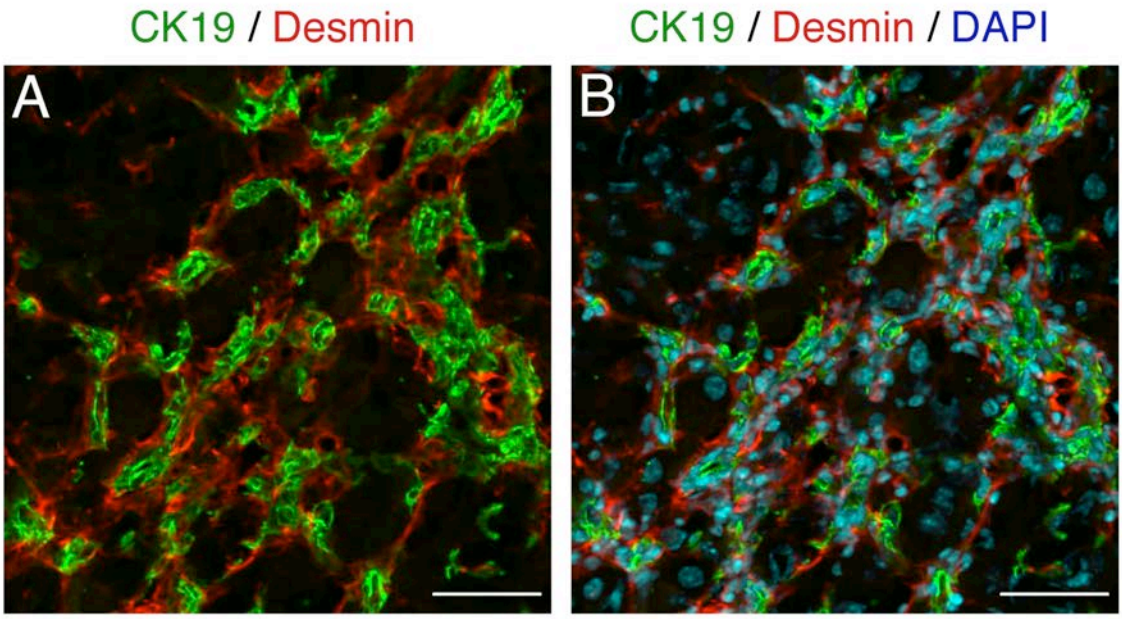

Supplemental Figure 6 Confocal microscopic analyses show that TAA-induced biliary lineage cells around the central veins in the liver are distinct from surrounding stellate cells. (**A** and **B**) Co-immunofluorescence staining of CK19 and desmin in the liver was conducted after 14 weeks of TAA administration. DNA was stained with DAPI. Scale bars, 50 μm.

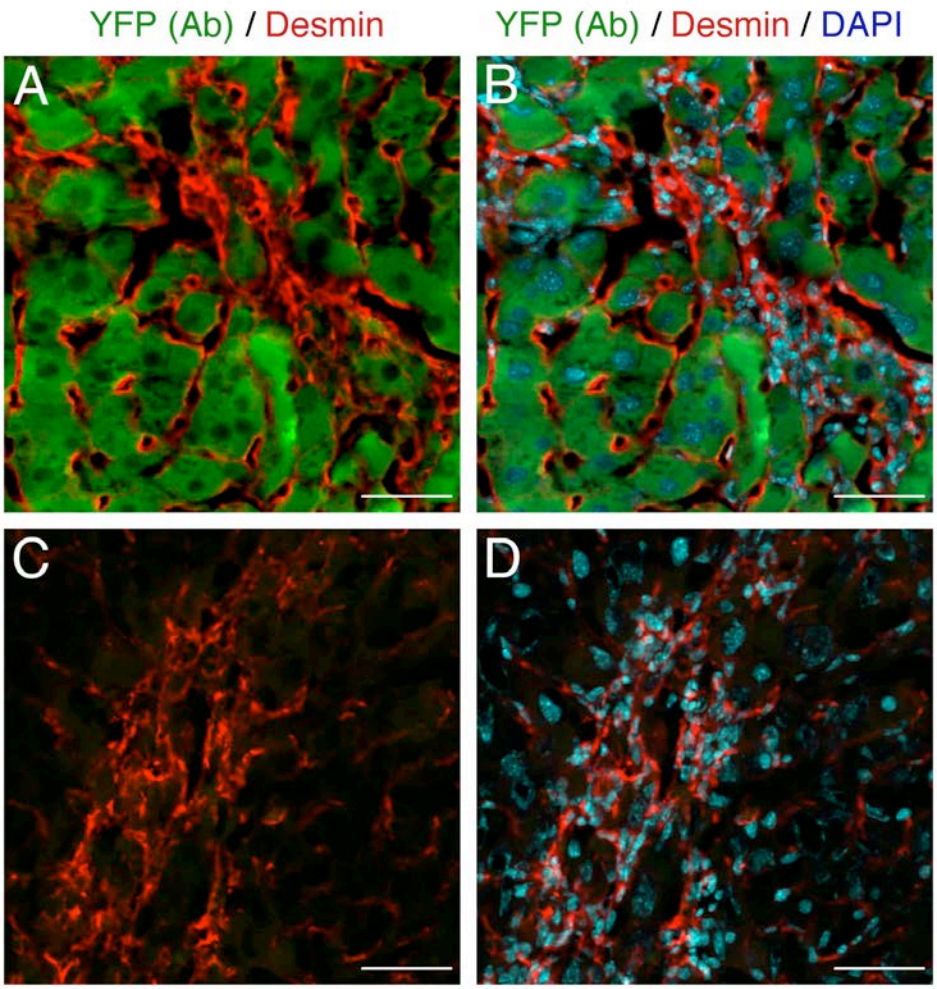

Supplemental Figure 7 Confocal microscopic analyses show that TAA does not induce unexpected Cre activity in stellate cells, regardless of the presence or absence of TM administration. (**A**–**D**) Co-immunofluorescence staining of YFP and desmin was conducted in the liver of *Alb-CreER*^{T2};*R26R*$^{YFP/+}$ mice after 14 weeks of TAA administration, with (**A** and **B**) or without (**C** and **D**) prior administration of TM. Ab: an anti-GFP/YFP antibody was used. DNA was stained with DAPI. Scale bars, 50 μm.

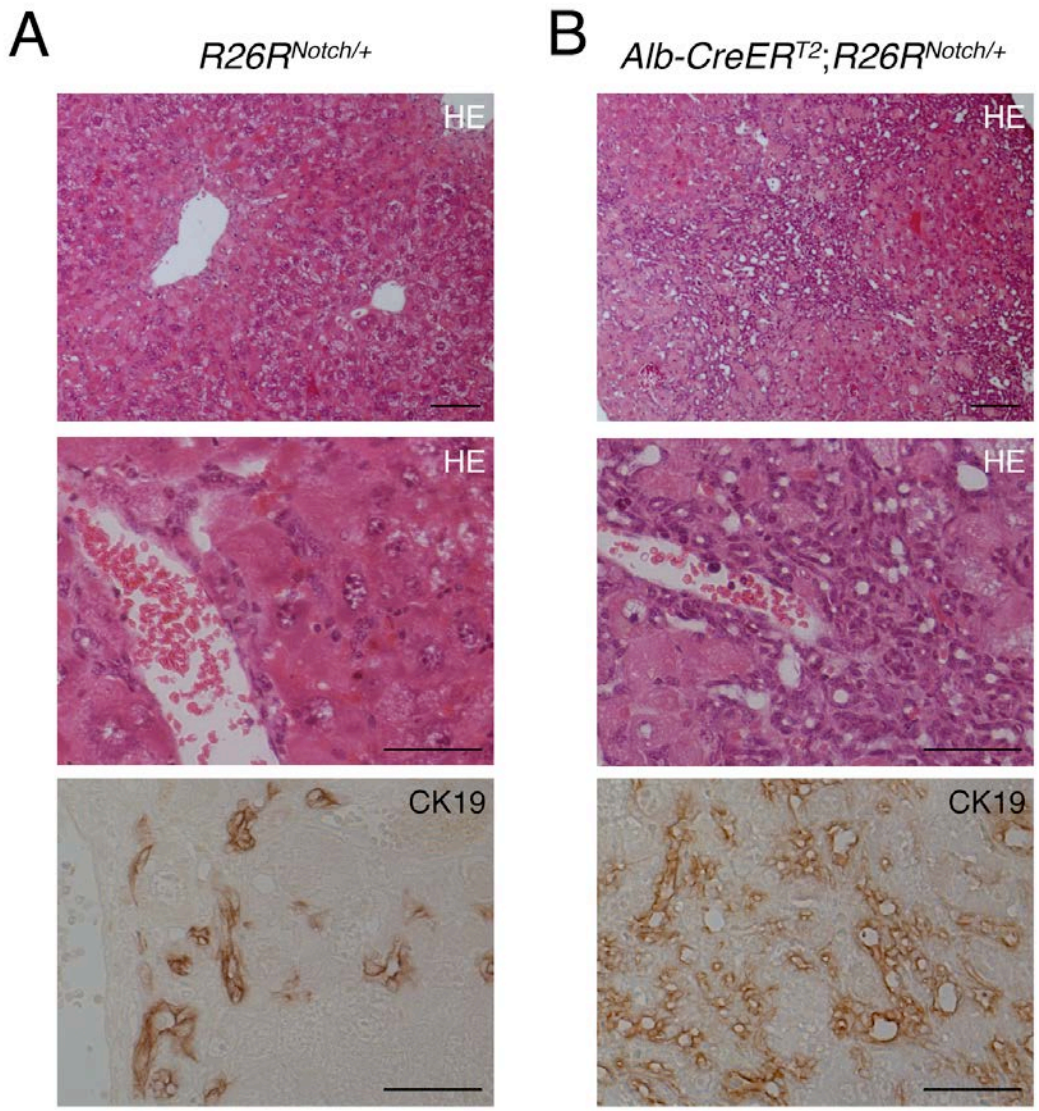

Supplemental Figure 8 The number of developing primitive ductules formed by TAA-induced biliary lineage cells is significantly increased when Notch signaling is activated in hepatocytes. (**A** and **B**) Hematoxylin and eosin (HE) staining and immunohistochemical staining of CK19 were conducted in the liver of *R26R*$^{Notch/+}$ (**A**) and *Alb-CreER*^{T2};*R26R*$^{Notch/+}$ (**B**) mice after 14 weeks of TAA administration. Scale bars, 100 μm (**A** and **B**, upper panels) and 50 μm (**A** and **B**, middle and bottom panels).

Supplemental Table 1. Notch activation is significant for neoplastic nodule formation after 14 weeks of TAA administration.

Mouse line	Nodule formation
R26R$^{Notch/+}$	0/5 (0%)
Alb-CreER^{T2};R26R$^{Notch/+}$	7/7 (100%)
Alb-CreER^{T2};Hes1$^{fl/fl}$	0/6 (0%)

Supplemental Table 1 Macroscopic nodule formation in the liver of the indicated mouse lines after 14 weeks of TAA administration.